A Class of Speed-Sensorless Sliding-Mode Observers for High-Performance Induction Motor Drives

Cristian Lascu, Ion Boldea, *Fellow, IEEE*, and Frede Blaabjerg, *Fellow, IEEE*

***Abstract*—A new family of speed-sensorless sliding-mode observers for induction motor drives has been developed. Three topologies are investigated in order to determine their feasibility, parameter sensitivity, and practical applicability. The most significant feature of all schemes is that they do not require the rotor speed adaptation, i.e., they are inherently sensorless observers. The most versatile and robust is a dual-reference-frame full-order flux observer. The other two schemes are flux observers implemented in stator frame and rotor frame, respectively. These are simpler than the first one and make use of the sliding-mode invariance over a specified range of modeling uncertainties and disturbances. Main theoretical aspects, results of parameter sensitivity analysis, and implementation details are given for each observer in order to allow the comparison. Experimental results with the dual-reference-frame observer, considered the most adequate for practical applications, are presented and discussed. Sensorless operation with a sliding-mode direct-torque-controlled drive at very low speeds is demonstrated. It is concluded that the new proposed observers represent a feasible alternative to the classical speed-adaptive flux observers.**

***Index Terms*—Sliding-mode observers (SMOs), state observers, variable-speed drives, variable-structure systems.**

I. Introduction

ADJUSTABLE-SPEED drives with induction motors (IMs) have already evolved as a mature technology. Accurate sensorless operation is possible at all speeds, except for the very low ones, where performances tend to be poor. State observers, employed as sensor replacements, are more reliable and affordable than the sensors they replace. A state observer is a real-time model of a real process or system, which produces an approximation of the state vector of that system and whose characteristics are somewhat free to be determined by the designer [1]. Usually, an observer has zero-lag filtering properties. Their accuracy and robustness in face of parameter detuning and perturbations are critical for the good operation of the drive [2].

For IM drives, the speed-adaptive observers are widely employed due to their accuracy. Most adaptive schemes are Luenberger observers [1]–[4], extended Kalman filters [5], [6], or sliding-mode observers (SMOs) [6]–[11]. In all cases, the rotor speed is used as adaptive quantity. Usually, the speed estimation is the last step of the estimation process, and it is affected by noise and errors. The speed estimator is driven by the observation error, and this causes a lagging estimate of the speed. When this inaccurate estimate is fed back to the observer, the flux estimation accuracy deteriorates, and side effects like limit cycles and/or noise sensitivity may appear, particularly at low speeds.

This paper presents the results of a research that attempted to answer a simple question: Is it possible to build observers which do not employ speed adaptation? Such an observer is referred to as an inherently sensorless observer and is expected to provide increased accuracy in a wide-speed-range operation and to have reduced overall complexity. In drives that do not use the rotor speed for other purposes (in torque-controlled drives), a sensorless observer leads to complete elimination of the speed estimator, and it is preferable to its adaptive counterpart. This paper compares three new sensorless observers for IM drives. The first one is a full-order SMO previously developed by the authors in [15]. The other two are new contributions proposed here. The main theoretical aspects, results of parameter sensitivity analysis, and implementation details are presented for each scheme. Representative experimental results with the observer, considered the most adequate for practical drive systems, are given and discussed.

II. Overview of Sensorless Observers

Although the most popular are the full-order speed-adaptive observers, several schemes, most of them of reduced order, have been developed without speed adaptation [11]–[16]. The well-known voltage-model-based estimator is inherently sensorless but is marginally stable due to the open-loop integration. The classical approach to maintain stability is to replace the integrator with a low-pass filter, a solution that fails at frequencies lower than several times the filter cutoff frequency.

A voltage-model-based observer for high-bandwidth operation with explicit compensation of the inverter nonlinearity, measurement offset, and noise is proposed in [12]. It includes a nonlinear offset estimator that forces the estimated stator-flux vector on a circular trajectory. Very low speed (7.5 r/min) sensorless operation was reported. This solution requires accurate knowledge of the inverter characteristics.

A current-model-based sensorless observer is reported in [11]. This is an SMO that is insensitive to the rotor time constant detuning, using a sliding function based on the estimated current error which approximates the rotor-flux derivative. Both

Manuscript received September 15, 2008; revised April 29, 2009. First published May 15, 2009; current version published August 12, 2009.

C. Lascu is with the Department of Electrical and Biomedical Engineering, University of Nevada, Reno, NV 89557 USA (e-mail: clascu@unr.edu).

I. Boldea is with the Faculty of Electrical Engineering, University Politehnica of Timisoara, 300223 Timisoara, Romania (e-mail: boldea@lselinux.upt.ro).

F. Blaabjerg is with the Institute of Energy Technology, Faculty of Engineering, Science and Medicine, Aalborg University, 9220 Aalborg, Denmark (e-mail fbl@iet.aau.dk).

Digital Object Identifier 10.1109/TIE.2009.2022518

rotor flux and speed are estimated from the sliding function. Low-speed sensorless operation at 20 r/min has been achieved.

Reduced-order observers, which combine the voltage and current models, are described in [13] and [14]. In both cases, the observer gain is selected so as to produce smooth transition from the current model to the voltage model as the speed increases. The observer in [13] reduces to inherently sensorless schemes for particular gain selections. The one in [14] and [16] is always sensorless, but the current model, used as virtual reference, is open loop operated, and it is prone to errors. Low-speed operation at 30 r/min was reported in both cases.

Full-order sensorless observers have not been realized yet, to our best knowledge. Usually, a full-order observer employs the time-variable motor models in stator [3] or rotor reference frame [4]. Although various reference frames and motor models may be used, the observer is always implemented in a single frame. Whatever the frame is, as long as full-order models are involved, at least one term of the model is rotor speed dependent and the observer must be speed adaptive.

Two conceptual approaches have been identified and investigated in this paper as potential solutions for the development of inherently sensorless observers:

1) by considering the back-EMF terms as disturbances and allowing the observer to estimate them in the same way as for any disturbance;
2) by using two reference frames to implement the motor model so as the speed-dependent back-EMF terms do not appear in the respective equations.

The first case takes advantage of the sliding-mode specific invariance over a specified range of modeling uncertainties in order to eliminate the speed-dependent EMF terms. All schemes benefit of the excellent sliding-mode robustness in face of parameter detuning and other disturbances. The new observers are analyzed next.

III. Stator-Flux-Model-Based Observer

A. Observer Synthesis

Dynamic models of real systems are defined using known characteristics of those systems, while the unknown ones are considered disturbances and are not included in the model. Ultimately, which characteristics are included or not within the model is a subjective choice of the designer and depends on the available information and technical and computational resources. The same reasoning applies for observers, whose structures may exhibit a large degree of flexibility [1]. Usually, an observer employs a real-time model of the plant, driven by the same inputs as the real system. A feedback controller is used to force the model to track the measured states. The plant model estimates the states with zero phase-lag due to the feedforward action provided by input quantities, while the controller estimates the disturbances with nonzero phase lag. The new observers presented next consider the speed-adaptive back-EMF terms as disturbances and implement a feedback sliding-mode controller that estimates them. Due to the sliding-mode invariance, the motor states will be accurately estimated.

The stator-flux-model-based observer (SFMO) uses the state-space motor model that has stator flux $\underline{\psi}_s$ and stator current $\underline{i}_s$ as state variables. In rotor reference frame, rotating with rotor speed ω_r, this model is

$$\frac{d}{dt}\underline{\psi}_s = -R_s\underline{i}_s - j\omega_r\underline{\psi}_s + \underline{u}_s \tag{1}$$

$$\frac{d}{dt}\underline{i}_s = -\left(\frac{1}{T_s\sigma}+\frac{1}{T_r\sigma}\right)\underline{i}_s + \frac{1}{L_s\sigma}\left(\frac{1}{T_r}-j\omega_r\right)\underline{\psi}_s + \frac{1}{L_s\sigma}\underline{u}_s \tag{2}$$

where $\underline{u}_s$ is the stator voltage vector; R_s and R_r are the stator and rotor resistances; L_s, L_r, and L_m are the stator, rotor, and magnetizing inductances; $T_s = L_s/R_s$; $T_r = L_r/R_r$; $\sigma = 1 - L_m^2/L_sL_r$; and $L_\sigma^2 = L_sL_r\sigma$.

Both equations contain the back-EMF $j\omega_r\underline{\psi}_s$. This term is considered as disturbance, and a controller that is able to estimate it has been designed. An inherently sensorless SMO based on model (1) and (2) is

$$\frac{d}{dt}\hat{\underline{\psi}}_s = -R_s\underline{i}_s + \underline{u}_s - K\underline{\nu} \tag{3}$$

$$\frac{d}{dt}\hat{\underline{i}}_s = -\left(\frac{1}{T_s\sigma}+\frac{1}{T_r\sigma}\right)\hat{\underline{i}}_s + \frac{1}{L_sT_r\sigma}\hat{\underline{\psi}}_s + \frac{1}{L_s\sigma}\underline{u}_s - \frac{1}{L_s\sigma}K\underline{\nu} \tag{4}$$

where K is the observer gain and the correction vector $\underline{\nu}$ is the output of a PI sliding-mode controller

$$\underline{\nu} = \operatorname{sgn}(S), \quad S = (K_P + K_I/s)(\underline{i}_s - \hat{\underline{i}}_s)) \tag{5}$$

where $s \equiv d/dt$, K_P and K_I are the PI gains, S is the sliding surface, and the *sign* function is component-wise applied to S. The PI controller has been included in order to impose the desired dynamics for the current estimation error. The sliding controller exhibits good robustness properties and system order reduction. In sliding modes, $S = 0$, $dS/dt = 0$, and for $K_I \neq 0$, the time constant of the current error dynamics is K_P/K_I. The equivalent control component of $K\underline{\nu}$ function approximates the back-EMF, i.e., $(K\underline{\nu})_{\text{eq}} = j\omega_r\underline{\psi}_s - \underline{e}_{\psi s}/T_r$, where $\underline{e}_{\psi s} = \underline{\psi}_s - \hat{\underline{\psi}}_s$.

The stability condition for current estimation obtained from Lyapunov analysis requires the observer gain to be large enough, so as to dominate the disturbance, i.e., $K > \max(|\omega_r\psi_s - e_{\psi s}/T_r|)$, for any operation point. The back-EMF is always bounded, and a value of $K \geq 300$ was adequate for the motor used. The stator-flux error dynamics, for $K_I = 0$, is of first order

$$\frac{d}{dt}\underline{e}_{\psi s} = -\frac{1}{T_r}\underline{e}_{\psi s}. \tag{6}$$

This indicates that T_r defines the convergence rate of the flux observer, and that rate is not tunable.

Some improvements may be considered. The value of $K = 300$ is conservative and causes moderate chattering. By using the saturation function in place of sign function, the chattering was significantly reduced. If the drive uses speed control,

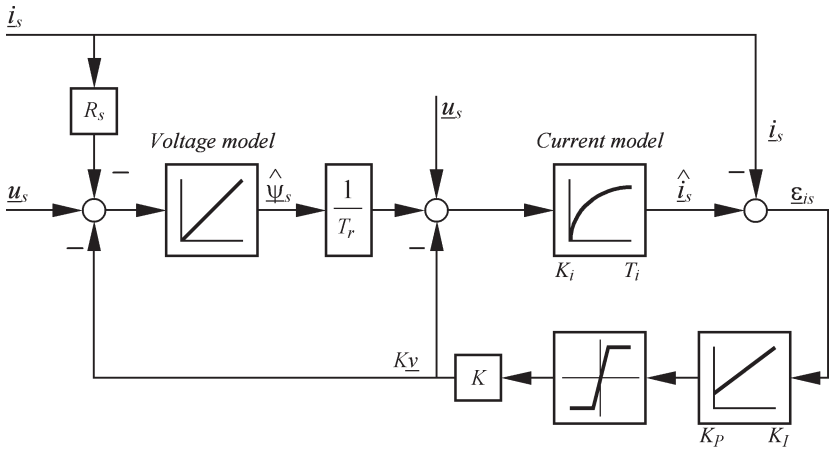

Fig. 1. Stator-flux-model-based inherently sensorless observer, SFMO.

K may be modified in accordance to reference speed, small for low speeds, and large for high speeds, taking provisions to fulfill the stability condition at any operation point. In this way, the chattering can be further reduced at low speeds.

A block diagram of the inherently sensorless SFMO is shown in Fig. 1, where $K_i = 1/(R_s + L_s/T_r)$, and $T_i = L_s\sigma \cdot K_i$ are the gain and time constant of the current model (4). If the rotor flux is needed, it can be calculated with (19). All quantities are in rotor reference frame. For simplicity, the coordinate transformations have been omitted from Fig. 1. This scheme is simple and linear but requires the knowledge of the rotor position. Therefore, it is best applicable in drives that use some form of rotor position estimation or a position measurement device.

B. Parameter Sensitivity Analysis

The sliding mode is known to be robust with respect to parameter detuning and modeling errors. However, some parameters, like the resistances, are variable in a rather wide range. Parameter sensitivity analysis, by means of simulation, has been carried out in order to determine the actual robustness of SFMO. The SFMO was integrated within a variable-structure direct-torque-controlled (DTC) drive. The following torque and speed profiles have been applied for all simulations.

1) *Speed profile*: $t = 0{-}2$ s: startup followed by high-speed operation at 300 rad/s; $t = 2{-}4$ s: deceleration and low-speed operation at 3 rad/s.
2) *Load torque*: $t = 0{-}1$ s: no load; $t = 1{-}4$ s: full-load (7-N $\cdot$ m) operation.

The observer gains are $K = 300$, $K_P = 1$, and $K_I = 1000$, and the saturation function, instead of the sign function, was employed in (5) in order to reduce the chattering during the sliding modes. Initial conditions are zero for all quantities. Observer convergence rate is not relevant for this particular application since the drive operation is disabled when the estimation errors are too large.

The SFMO is insensitive to stator resistance detuning, as shown in Fig. 2 which gives the stator-flux magnitude and phase errors for -50% R_s error. Similar results have been obtained for positive errors and for the rotor flux. This outcome was

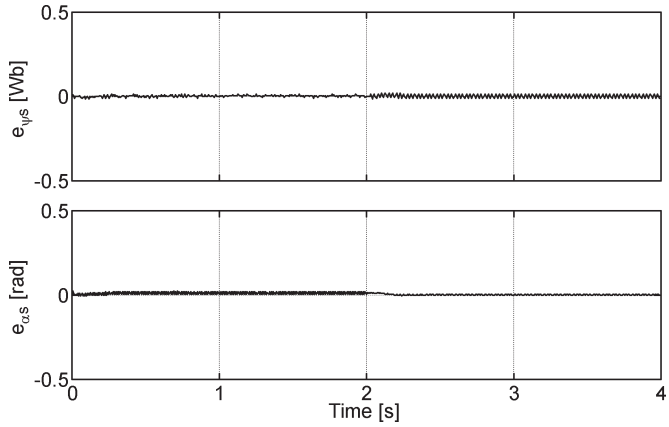

Fig. 2. Stator-flux magnitude and phase errors for -50% R_s detuning.

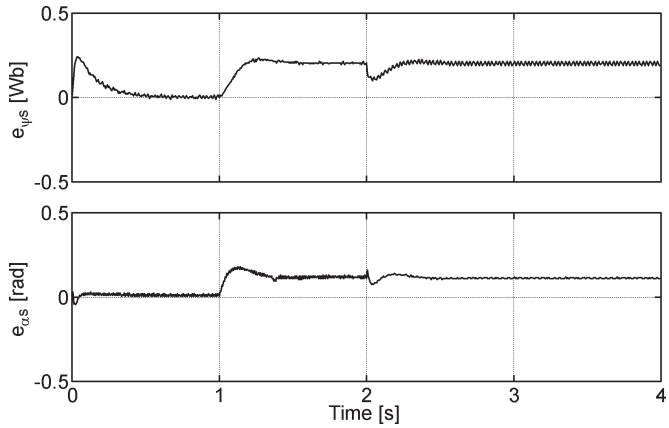

Fig. 3. Stator-flux magnitude and phase errors for -25% R_r detuning.

expected since the resistive voltage drop $R_s i_s$ appears in (3) and (4), with the same sign and the same gain as the assumed disturbance.

The sensitivity to rotor resistance detuning is shown in Fig. 3, which shows the same errors for -25% R_r detuning. The estimation is compromised at all speeds when the torque is nonzero. Stable operation was not possible for errors larger than 25%.

The sensitivity of SFMO to magnetizing inductance detuning is shown in Fig. 4 for -25% L_m error. At this time, the no-load

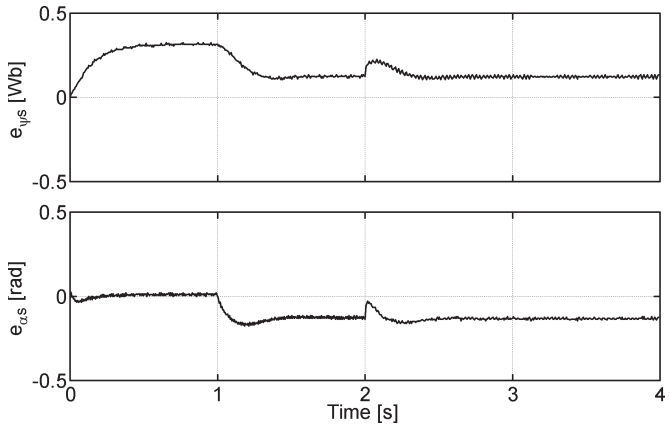

Fig. 4. Stator-flux magnitude and phase errors for -25% L_m detuning.

operation is mostly affected, while in loaded operation, the errors are smaller. Increasing the gain K does not help in reducing these errors, neither for R_r nor for L_m detuning. This result was expected since the rotor resistance and the magnetizing inductance are only present in the current-model equation (4). Thus, (4) alone needs the compensation for these parameters, while the feedback correction $K\underline{\nu}$, which compensates for all disturbances present in the model, is applied to (3) and (4). Although not shown, the current error was always zero.

Overall, the SFMO is not very well suited for practical implementation because it does not offer many advantages. It requires the knowledge of the rotor position and, despite correct orientation, shows severe sensitivity to rotor resistance and magnetizing inductance detuning.

IV. Rotor-Flux-Model-Based Observer

A. Observer Synthesis

An inherently sensorless observer in stator reference frame can be realized in a similar way as the SFMO by using the rotor-flux motor model (7) and (8). This model is in the stator reference frame and has the rotor flux $\underline{\psi}_r$ and the stator current $\underline{i}_s$ as state variables.

$$\frac{d}{dt}\underline{\psi}_r = \frac{L_m}{T_r}\underline{i}_s + \left(j\omega_r - \frac{1}{T_r}\right)\underline{\psi}_r \tag{7}$$

$$\frac{d}{dt}\underline{i}_s = \frac{1}{L_s\sigma}\left(-R_s - \frac{L_m^2}{L_rT_r}\right)\underline{i}_s + \frac{L_m}{L_\sigma^2}\left(\frac{1}{T_r} - j\omega_r\right)\underline{\psi}_r + \frac{1}{L_s\sigma}\underline{u}_s. \tag{8}$$

Both equations contain the back-EMF term $j\omega_r\underline{\psi}_r$. This term is considered as disturbance, and an estimator has been designed for it. An inherently sensorless SMO based on model (7) and (8) is

$$\frac{d}{dt}\hat{\underline{\psi}}_r = \frac{L_m}{T_r}\underline{i}_s - \frac{1}{T_r}\hat{\underline{\psi}}_r + K\underline{\nu} \tag{9}$$

$$\frac{d}{dt}\hat{\underline{i}}_s = \frac{1}{L_s\sigma}\left(-R_s - \frac{L_m^2}{L_rT_r}\right)\hat{\underline{i}}_s + \frac{L_m}{L_\sigma^2T_r}\hat{\underline{\psi}}_r + \frac{1}{L_s\sigma}\underline{u}_s - \frac{L_m}{L_\sigma^2}K\underline{\nu} \tag{10}$$

where K is the observer gain and the correction vector $\underline{\nu}$ is the output of a PI sliding-mode controller

$$\underline{\nu} = \mathrm{sgn}(S), \quad S = (K_P + K_I/s)(\underline{i}_s - \hat{\underline{i}}_s). \tag{11}$$

During sliding mode $S = 0$, $dS/dt = 0$, and the equivalent control component of the function $K\underline{\nu}$ approximates the back-EMF, i.e., $(K\underline{\nu})_{\mathrm{eq}} = j\omega_r\underline{\psi}_r - \underline{e}_{\psi r}/T_r$, $\underline{e}_{\psi r} = \underline{\psi}_r - \hat{\underline{\psi}}_r$. The stability condition for current estimation is similar, $K > \max(|\omega_r\psi_r - e_{\psi r}/T_r|)$, and a value of $K \geq 300$ is adequate. The chattering that accompanies the sliding mode can be reduced by using the saturation function and by implementing a speed-dependent gain.

The rotor-flux error dynamics, for $K_I = 0$, is

$$\frac{d}{dt}\underline{\psi}_r = 0. \tag{12}$$

This represents the dynamics of an integrator, which causes instability in the presence of measurement offset. In order to avoid this problem, an offset estimator based on the min–max approach, as described in [12], may be implemented in a real drive.

A block diagram of the rotor-flux-model-based observer (RFMO) is shown in Fig. 5, where $K_v = L_\sigma^2T_r/(L_rT_rR_s + L_m^2)$ and $T_v = K_v$ are the gain and time constant of the voltage model (10). If stator flux is needed, it can be calculated with (19). All quantities in Fig. 5 are in stator frame, and no coordinate transformations are needed. This scheme is simpler than the SFMO, and its sensitivity to parameter detuning is lower. Both the SFMO and RFMO offer the advantage that, when needed, a rotor speed estimate is easily obtainable from the $K\underline{\nu}$ signal via low-pass filtering and algebraic calculations, assuming $\underline{e}_{\psi s} = 0$ or $\underline{e}_{\psi r} = 0$.

B. Parameter Sensitivity Analysis

Simulations with the RFMO have been performed in order to determine the sensitivity to parameter detuning. Identical operating conditions and the same gains as in the case of the SFMO were employed.

The RFMO is sensitive to stator resistance detuning, as can be noticed in Fig. 6, which shows the stator-flux magnitude and phase errors for -25% R_s detuning. Errors are large at low speeds and moderate at high speeds. The sensitivity is more severe than for dual reference frame observer (DRFO) (next section), which is sensitive to R_s at low speeds only. As detuning magnitude increases, the drive becomes unstable, particularly for positive R_s errors.

The RFMO is insensitive to rotor resistance and to magnetizing inductance detuning, as can be noticed in Figs. 7 and 8, which show the stator-flux magnitude and phase errors for -50% R_r error and -50% L_m error, respectively. In all cases, similar results have been obtained for positive detuning and for the rotor flux. In the case of L_m detuning, the rotor-flux magnitude shows only a very small error. Both parameters R_r and L_m are present in both equations of the model (9) and (10), and the compensation function $K\underline{\nu}$ is able to correctly estimate

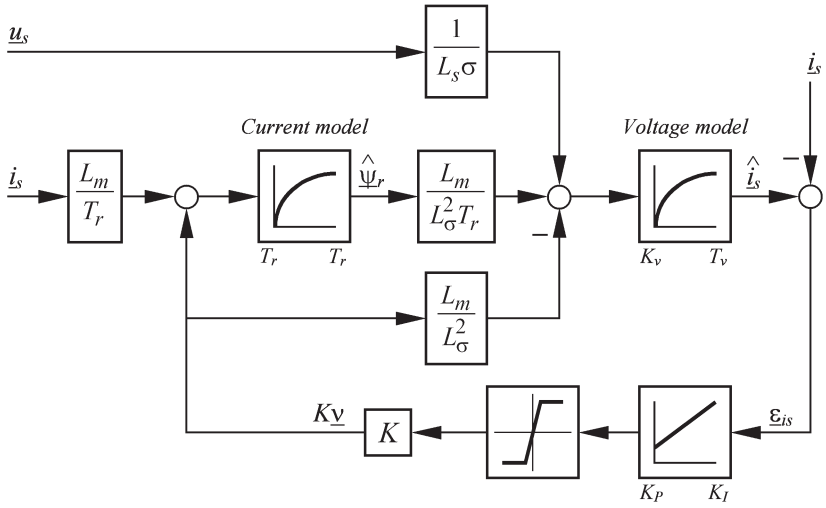

Fig. 5. Rotor-flux-model-based inherently sensorless observer, RFMO.

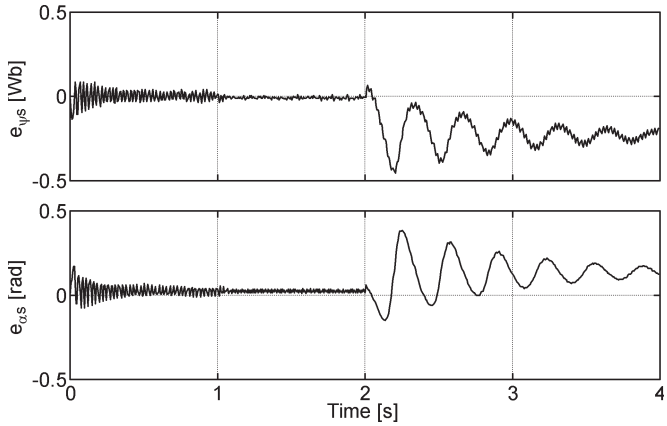

Fig. 6. Stator-flux magnitude and phase errors for -25% R_s detuning.

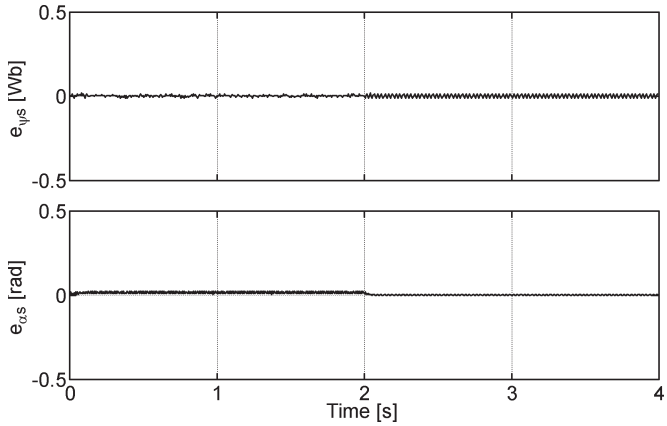

Fig. 7. Stator-flux magnitude and phase errors for -50% R_r detuning.

the errors. Not so for R_s detuning, which is present in (10) only. A stator resistance estimator is desirable for RFMO.

Overall, the RFMO has good performance, comparable to that of the DRFO. Its topology is simple, without use of coordinate transformations, and accompanied by a stator resistance estimator and an offset compensator, it is a serious candidate for a sensorless observer position in high-performance drives.

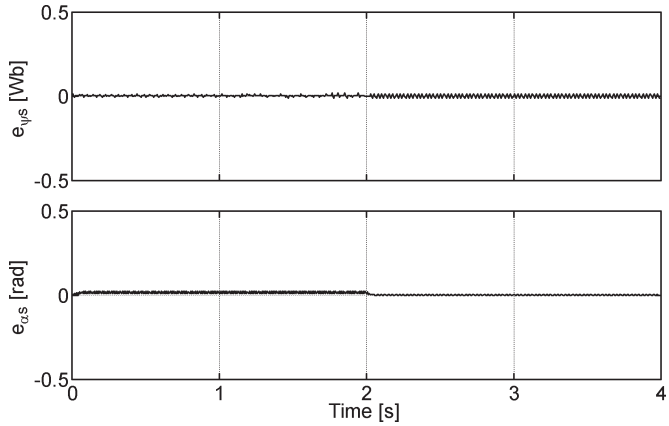

Fig. 8. Stator-flux magnitude and phase errors for -50% L_m detuning.

V. Dual Reference Frame Observer

A. Observer Synthesis

The dual reference frame observer employs two reference frames, so that the speed-dependent terms within the motor model do not appear in its implementation. This approach is based on the state-space model that has the stator flux $\underline{\psi}_s$ and the rotor flux $\underline{\psi}_r$ as state variables. In a reference frame rotating with arbitrary speed ω_e, the model is

$$\frac{d}{dt}\underline{\psi}_s = -\left(\frac{1}{T_s\sigma} + j\omega_e\right)\underline{\psi}_s + \frac{L_m}{L_r T_s \sigma}\underline{\psi}_r + \underline{u}_s \quad (13)$$

$$\frac{d}{dt}\underline{\psi}_r = \frac{L_m}{L_s T_r \sigma}\underline{\psi}_s - \left(\frac{1}{T_r\sigma} + j(\omega_e - \omega_r)\right)\underline{\psi}_r. \quad (14)$$

The stator-flux equation (13) is independent of ω_e if it is implemented in stator frame or stator-flux reference frame. The rotor-flux equation (14) is independent of both ω_e and ω_r if it is implemented in rotor frame or rotor-flux reference frame.

A full-order observer with (13) in stator frame ($\omega_e = 0$) and (14) in rotor-flux frame (superscript "r"), rotating with

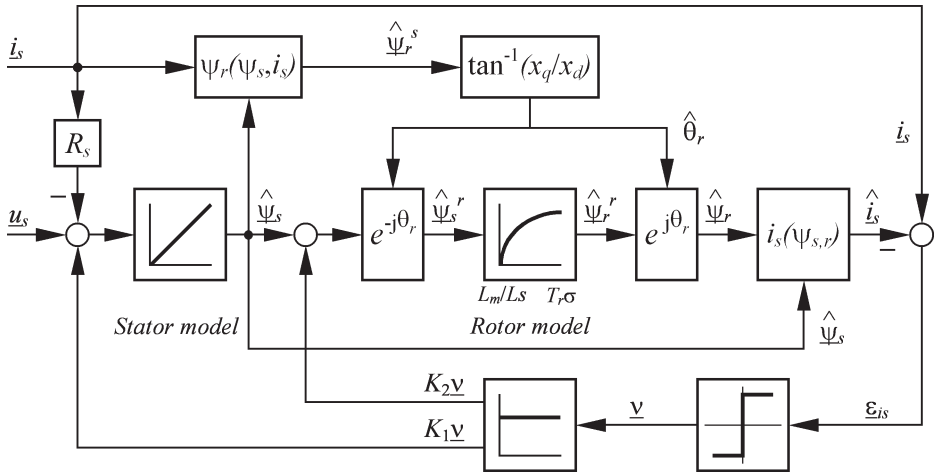

Fig. 9. Dual reference frame inherently sensorless observer, DRFO.

rotor-flux speed ($\omega_e = \omega_{\psi r}$), is

$$\frac{d}{dt}\hat{\underline{\psi}}_s = -\frac{1}{T_s\sigma}\hat{\underline{\psi}}_s + \frac{L_m}{L_rT_s\sigma}\hat{\underline{\psi}}_r + \underline{u}_s + K_1\underline{\nu} \quad (15)$$

$$\frac{d}{dt}\hat{\underline{\psi}}_r^r = \frac{L_m}{L_sT_r\sigma}\hat{\underline{\psi}}_s^r - \left(\frac{1}{T_r\sigma} + j(\omega_{\psi r}-\omega_r)\right)\hat{\underline{\psi}}_r^r + K_2\underline{\nu}^r \quad (16)$$

where $\underline{\nu}$ is the correction vector, $K = [K_1 \quad K_2]^{\mathrm{T}}$ is the observer gain, and superscript "^" denotes estimated variables. In the rotor-flux frame, the rotor-flux vector is $\underline{\psi}_r = \psi_{rd}$, and the real component of (16) is independent of $\omega_{\psi r}$ and ω_r. The observer is sensorless since it implements the real component of (16) and uses $\hat{\psi}_{rq} = 0$.

The correction mechanism is of sliding-mode type based on the estimation error of stator current $\underline{i}_s$

$$\underline{\nu} = \mathrm{sgn}(i_{sd} - \hat{i}_{sd}) + j\,\mathrm{sgn}(i_{sq} - \hat{i}_{sq}) \quad (17)$$

$$\hat{\underline{i}}_s = (L_r\hat{\underline{\psi}}_s - L_m\hat{\underline{\psi}}_r)/L_\sigma^2. \quad (18)$$

The gains K_1 and K_2 are complex values with reference speed-dependent imaginary components: $K_1 = k_{1d} + j\omega_r^* k_{1q}$ and $K_2 = k_{2d} + j\omega_r^* k_{2q}$. Similar results may be obtained with constant gains. A PI sliding surface may be used in (17) in the same way as in (11). The scheme can be simplified by substituting the rotor flux (19) in (15). In this way, the stator equation becomes the voltage model (20)

$$\hat{\underline{\psi}}_r = \left(L_r\hat{\underline{\psi}}_s - L_\sigma^2\underline{i}_s\right)/L_m \quad (19)$$

$$\frac{d}{dt}\hat{\underline{\psi}}_s = -R_s\underline{i}_s + \underline{u}_s + K_1\underline{\nu}. \quad (20)$$

During sliding mode $S = \underline{i}_s - \hat{\underline{i}}_s = 0$, $dS/dt = 0$ and $\nu = 0$. The stator-flux error dynamics for constant gains is given by (21) and the stability condition is given by (22)

$$\frac{d}{dt}e_{\psi s} = -K_1\nu = 0 \quad (21)$$

$$K_1L_r - K_2L_m > \max\left(|a\psi_s + b\psi_r|\right) \quad (22)$$

where $b = (L_r/L_s + L_m/L_r)L_m/T_r\sigma + j\omega_r L_m$ and $a = -L_r/T_s\sigma - L_m^2/L_rT_s\sigma$. Equation (22) gives a degree of freedom in choosing K_1 and K_2. Fine-tuning for these gains has been performed in the simulation.

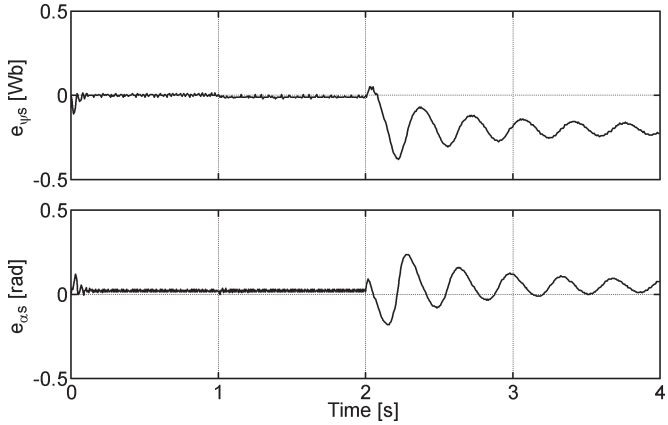

Fig. 10. Stator-flux magnitude and phase errors for -25% R_s detuning.

The DRFO implements (16)–(20) and its block diagram is shown in Fig. 9. The rotor-flux vector position is computed from the estimated rotor flux (19) in the stator reference, as shown in the upper side of Fig. 9.

This selection of reference frames was considered the most advantageous for a real drive. Other frames may be employed as well. If the rotor position is available, but the speed information is not needed, the rotor-flux equation may be implemented in the rotor frame. In this case, the block diagram in Fig. 9 remains the same, except for the rotor-flux position calculation, which may be omitted.

B. Parameter Sensitivity Analysis

The most important disturbances that affect observer accuracy are the parameter detuning, modeling errors, and measurement noise. The sliding-mode topology has been selected in order to increase the robustness with respect to these disturbances. The DRFO sensitivity to parameter detuning has been investigated by means of simulation. Similar operating conditions have been simulated.

The DRFO sensitivity to stator resistance detuning is shown in Fig. 10, which shows the stator-flux magnitude and phase estimation errors for -25% detuning of R_s. High-speed

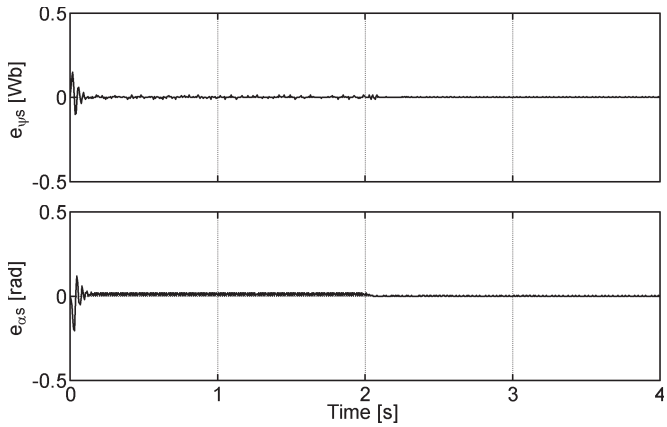

Fig. 11. Stator-flux magnitude and phase errors for -50% R_r detuning.

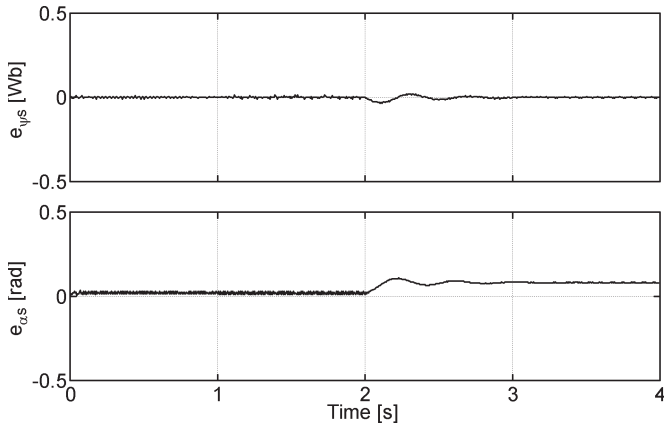

Fig. 12. Stator-flux magnitude and phase errors for $+50\%$ L_m detuning.

operation is not much affected, but the low-speed operation is ruined. Errors larger than 25% in R_s cause instability in sensorless operation. Increasing the observer gain K significantly reduces the error but increases the chattering associated with the sliding mode. The best way to manage the resistance sensitivity is to use a stator resistance estimator [see (23)].

The stator resistance is online adapted as

$$\hat{R}_s = R_{s0} - K_{Rs} \int_0^t (\hat{\psi}_{rd}\nu_q - \hat{\psi}_{rq}\nu_d)dt \tag{23}$$

where ν_d and ν_q are the components of (17).

The sensitivity to rotor resistance detuning for -50% error in R_r is shown in Fig. 11. The DRFO is practically insensitive to rotor resistance detuning. Small errors can be noticed at startup only, due to rotor time constant detuning. For both resistances, similar results have been obtained for the rotor flux and for positive detuning.

The same estimation errors for magnetizing inductance detuning are shown in Fig. 12, for $+50\%$ L_m error, and in Fig. 13, for -50% L_m error. The DRFO is robust to L_m overestimation at all speeds. Small phase error occurs at low speeds, but this has low impact on the drive behavior. Since underestimation of L_m produces inaccurate estimation, the overestimation of L_m is highly preferable whenever its value is uncertain. It turns out that DRFO has similar parameter sensitivity to an adaptive full-order observer. However, due to

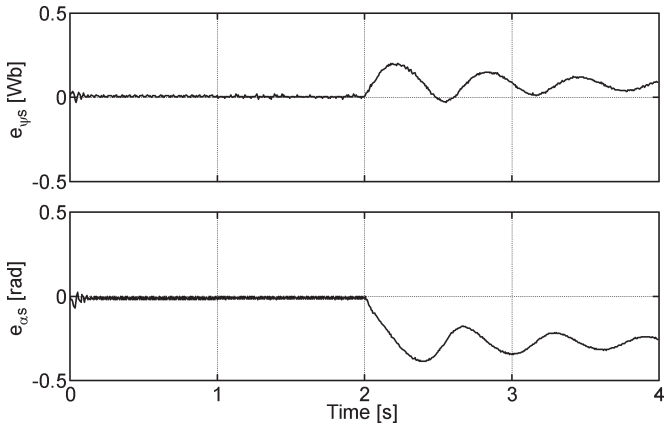

Fig. 13. Stator-flux magnitude and phase errors for -50% L_m detuning.

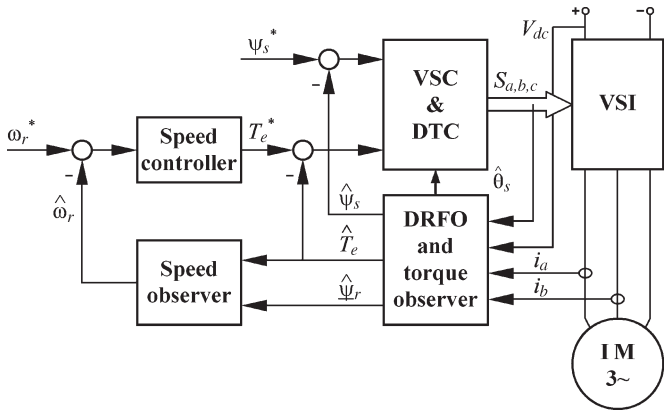

Fig. 14. VSC-DTC IM drive.

sliding mode, the estimation errors are smaller for the same level of detuning.

VI. Experimental Results

Experiments with the DRFO have been performed. This scheme has been considered the most appropriate for this phase of the research due to its flexibility and robustness. It displays very low offset sensitivity, and a stator resistance estimator was already available for it. The DRFO was integrated within a variable-structure control DTC (VSC-DTC) sensorless drive. A block diagram of this drive is shown in Fig. 14. Apart from the DRFO, the scheme contains torque and speed observers, the stator resistance estimator, a PI speed controller, and the VSC-DTC [15]. As described in [15], VSC-DTC applies the VSC concepts [7] to IM drives control. It is a switching torque and flux controller that receives as inputs the torque and flux errors, as shown in Fig. 14. All flux and speed observers are general-purpose observers; they may be used for any control strategy, not only for DTC.

The speed estimator used for all experiments is

$$\hat{\omega}_m = \hat{\omega}_r - \hat{\omega}_{sl} = \frac{1}{\hat{\psi}_r^2}\left(\frac{d\hat{\psi}_{r\beta}}{dt}\hat{\psi}_{r\alpha} - \frac{d\hat{\psi}_{r\alpha}}{dt}\hat{\psi}_{r\beta}\right) - \frac{L_m}{T_r}\frac{i_{sq}}{\hat{\psi}_r} \tag{24}$$

where ψ_r is (19), ω_r is its speed, and T_e is the torque.

Observer gains are $K = [20 + j0.1\omega_r^* - 10 + j0.1\omega_r^*]$, the same as used for simulations. It uses the reference speed ω_r^*.

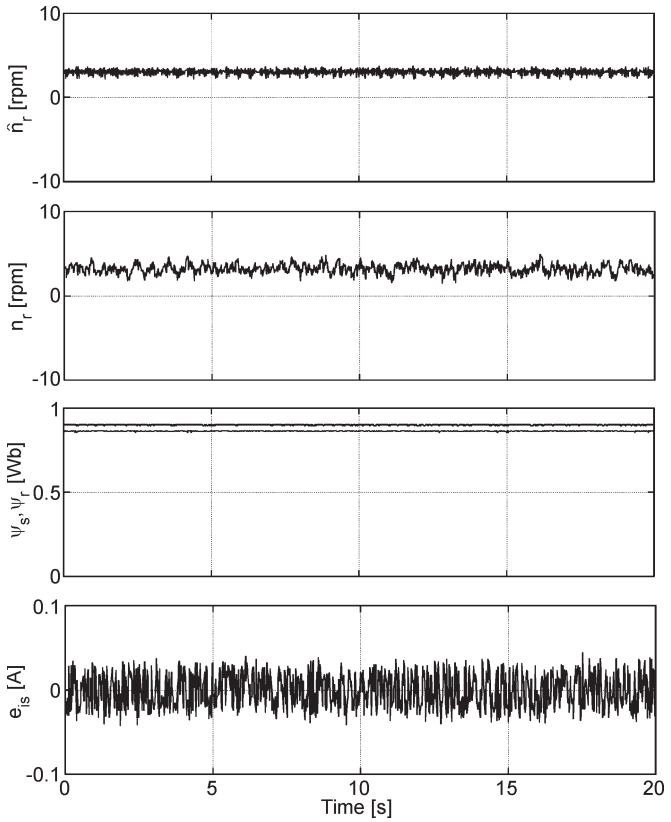

Fig. 15. Full-load sensorless operation at 3 r/min with DRFO. From top to bottom: estimated and measured speed, estimated stator- and rotor-flux magnitudes, and current estimation error.

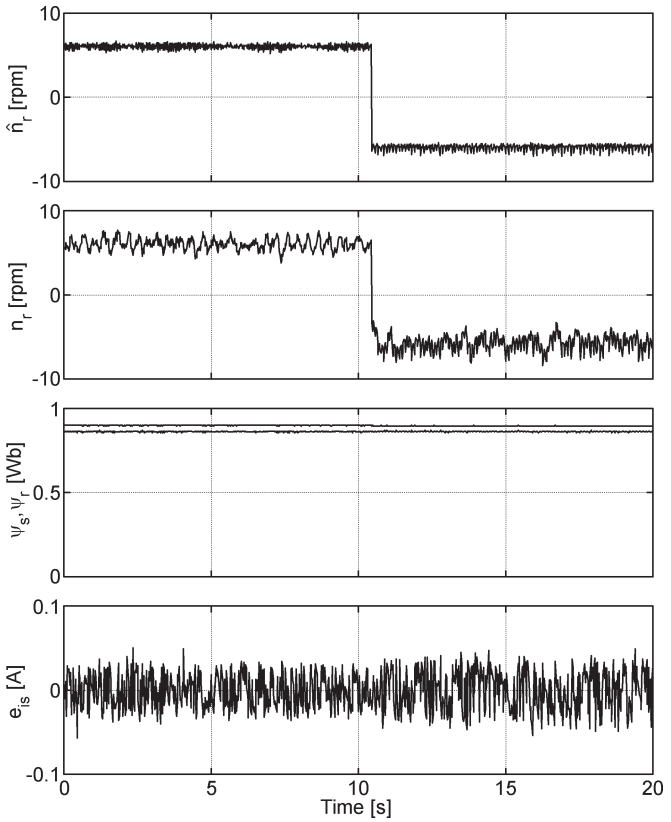

Fig. 16. Full-load sensorless reversal at 6 r/min with DRFO. From top to bottom: estimated and measured speed, estimated stator- and rotor-flux magnitudes, and current estimation error.

The drive employs a 4.3-kVA VLT5004 inverter from Danfoss Drives, Denmark. Inverter dead time and voltage drop were software compensated. The IM nameplate data and parameters are as follows: $P_N = 1.1$ kW, $U_{sN} = 380$ V, $f_{sN} = 50$ Hz, $n_N = 1475$ r/min, $p = 2$, $T_{eN} = 7$ N $\cdot$ m, $R_s = 5.46\ \Omega$, $R_r = 4.45\ \Omega$, $L_s = L_r = 0.492$ H, and $L_m = 0.475$ H. The motor was mechanically connected to a dc machine with capabilities of producing load torque at all speeds. A 5000-line encoder was used for speed monitoring only. The control hardware uses a dual-processor system with the ADSP-21062 and the ADMCF328 DSP-s from Analog Devices. Sampling and switching frequencies are 10 kHz.

Experiments were focused on the low-speed-operation performance, since this is one of the most challenging tests for a sensorless drive. The first experiment demonstrates full-load sensorless operation at 3 r/min (0.1-Hz electrical reference). Fig. 15 shows the estimated and real speeds, stator- and rotor-flux magnitudes, and current estimation error. Since real fluxes were not measured, the observation accuracy was valued on the base of speed and current estimation errors. The estimated speed replicates well the measured one, and its ripple is small. This is an indication that the flux observer is also accurate, since the speed was calculated from the rotor-flux estimate. The current error is also small, confirming the correct sliding-mode operation of DRFO.

Chattering due to the SMO operation is apparent in Fig. 15, but this does not significantly affect the drive operation or the estimation. The flux magnitudes and the estimated torque have low high-frequency noise content, much lower than a conventional DTC drive. Acoustical noise produced by the drive was insignificant. Overall, the amount of chattering was not a matter of concern for this application.

The second experiment shows sensorless motoring and braking operation at ± 6 r/min (± 0.2-Hz electrical reference) in Fig. 16. The machine runs for 10.5 s at $+6$ r/min, full-load, in motoring mode, and then, it is reversed to -6 r/min, while the torque is maintained almost unchanged (braking mode). Fig. 16 shows the estimated and real speeds, stator- and rotor-flux magnitudes, and current estimation error. Again, the estimated speed matches well the measured one in both regimes. During the reversal, the current estimation error remains bounded between ± 0.05-A limits, and the flux magnitude is insensitive to speed transients, indicating that the observer is not much affected by the reversal.

Other experiments at very low speeds, including stable operation at 0 r/min, have also been carried out. For all these extreme conditions, the speed ripple is small (motor rated speed is 1475 r/min), as noticed in Figs. 15 and 16.

The last experiment shows transient behavior of the drive during a startup to 1500 r/min. Before $t = 0$, the motor was not supplied. At $t = 0$, the stator-flux reference was set to 0.9 Wb, and after 10 ms, the speed reference was set to 1500 r/min. Speed, torque, and flux magnitude transients during the first half-second of the startup are shown in Fig. 17. The torque is limited at 12 N $\cdot$ m, and the speed increases linearly. The current estimation error is similar to e_{is} in Figs. 15 and 16. Accurate torque and flux control can be noticed, and their ripple is much smaller than in a conventional DTC drive.

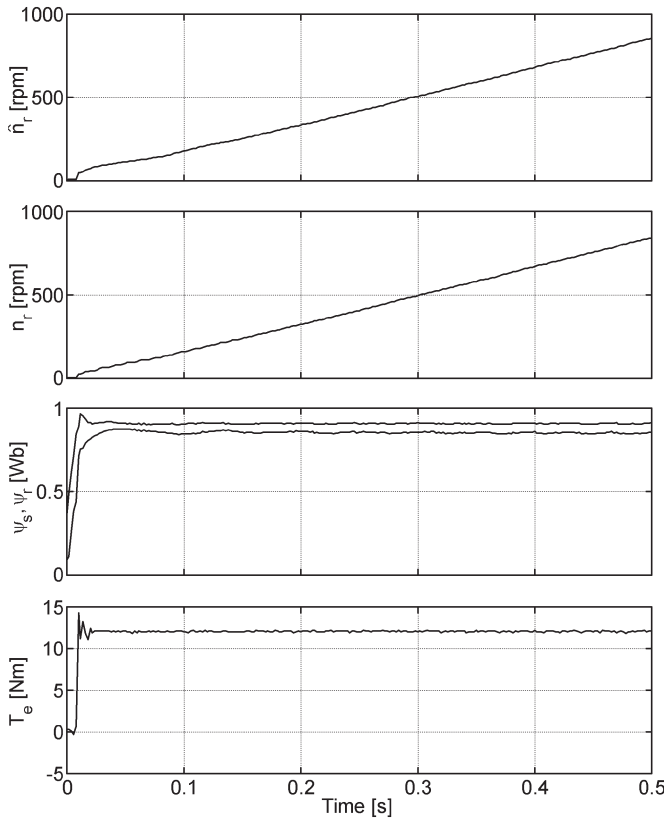

Fig. 17. Startup with DRFO. From top to bottom: Estimated and measured speed, estimated stator- and rotor-flux magnitudes, and estimated torque.

TABLE I
OBSERVER COMPARISON SUMMARY

Observer	DRFO	SFMO	RFMO
Complexity	High	Low	Medium
R_s sensitivity	High	No	High
R_r sensitivity	No	High	No
L_m sensitivity	Low	High	No

Overall, the VSC-DTC drive with DRFO displays very good performance in wide-speed-range operation—the highest speed tested was 3000 r/min. All experiments confirmed that the sliding-mode flux observer is very robust with respect to torque and speed transients.

VII. CONCLUSION

A class of inherently sensorless full-order sliding-mode observers for IM drives has been proposed and investigated in order to determine their performances. All are new schemes or have been previously developed by the authors. The analysis is focused on theoretical analysis and on comparison of the three schemes in terms of parameter sensitivity. As summarized in Table I, the observers have the following significant properties.

The DRFO has the most complex structure. It is sensitive to stator resistance detuning and to underestimation of magnetizing inductance. It is insensitive to rotor resistance errors and shows small sensitivity to magnetizing inductance overestimation. Online adaptation of stator resistance has been implemented. This observer is appropriate for practical implementation, and it has been extensively tested in a sliding-mode DTC drive.

The SFMO is simpler but requires knowledge of the rotor position. It is insensitive to stator resistance detuning but shows high sensitivity to rotor resistance and magnetizing inductance errors. Therefore, this inherently sensorless sliding observer is less attractive for practical implementation in a sensorless drive.

The RFMO has the simplest structure. It is sensitive to stator resistance detuning and to measurement offset and is insensitive to rotor resistance and magnetizing inductance errors. It is appropriate for practical implementation, provided that online adaptation of stator resistance and offset compensation are employed. Comparison of the SFMO and RFMO with respect to other inherently sensorless observers will be carried out in a future paper.

Very low speed sensorless operation was demonstrated with the DRFO in a VSC-DTC drive. To our best knowledge, 3 r/min is the lowest speed ever reported in sensorless operation without signal injection. This was possible due to the excellent robustness and high accuracy of the sliding-mode flux observer.

REFERENCES

[1] D. G. Luenberger, "An introduction to observers," *IEEE Trans. Autom. Control*, vol. AC-16, no. 6, pp. 596–602, Dec. 1971.
[2] R. D. Lorenz, "Observers and state filters in drives and power electronics," in *Conf. Rec. OPTIM*, May 2002, vol. 2, pp. 4–12.
[3] H. Kubota, K. Matsuse, and T. Nakano, "DSP based speed adaptive flux observer for induction motor applications," *IEEE Trans. Ind. Appl.*, vol. 29, no. 2, pp. 344–348, Mar./Apr. 1993.
[4] J. Maes and J. Melkebeek, "Speed-sensorless direct torque control of induction motors using an adaptive flux observer," *IEEE Trans. Ind. Appl.*, vol. 36, no. 3, pp. 778–785, May/Jun. 2000.
[5] Y.-R. Kim, S.-K. Sul, and M.-H. Park, "Speed sensorless vector control of induction motor using extended Kalman filter," *IEEE Trans. Ind. Appl.*, vol. 30, no. 5, pp. 1225–1233, Sep./Oct. 1994.
[6] F. Chen and M. W. Dunnigan, "Comparative study of a sliding-mode observer and Kalman filters for full state estimation in an induction machine," *Proc. Inst. Elect. Eng.—Elect. Power Appl.*, vol. 149, no. 1, pp. 53–64, Jan. 2002.
[7] V. Utkin, J. Guldner, and J. Shi, *Sliding Mode Control in Electromechanical Systems*. New York: Taylor & Francis, 1999.
[8] Z. Yan, C. Jin, and V. I. Utkin, "Sensorless sliding-mode control of induction motors," *IEEE Trans. Ind. Electron.*, vol. 47, no. 6, pp. 1286–1297, Dec. 2000.
[9] Z. Yan and V. Utkin, "Sliding mode observers for electric machines—An overview," in *Conf. Rec. IEEE IECON*, Nov. 2002, vol. 3, pp. 1842–1847.
[10] M. Tursini, R. Petrella, and F. Parasiliti, "Adaptive sliding-mode observer for speed sensorless control of induction motors," *IEEE Trans. Ind. Appl.*, vol. 36, no. 5, pp. 1380–1387, Sep./Oct. 2000.
[11] H. Rehman, A. Derdiyok, M. K. Gûven, and L. Xu, "A new current model flux observer for wide speed range sensorless control of an induction machine," *IEEE Trans. Power Electron.*, vol. 17, no. 6, pp. 1041–1048, Nov. 2002.
[12] J. Holtz and J. Quan, "Sensorless vector control of induction motors at very low speed using a nonlinear inverter model and parameter identification," *IEEE Trans. Ind. Appl.*, vol. 38, no. 4, pp. 1087–1095, Jul./Aug. 2002.
[13] L. Harnefors, "Design and analysis of general rotor-flux-oriented vector control systems," *IEEE Trans. Ind. Electron.*, vol. 48, no. 2, pp. 383–390, Apr. 2001.
[14] C. Lascu, I. Boldea, and F. Blaabjerg, "A modified direct torque control for induction motor sensorless drive," *IEEE Trans. Ind. Appl.*, vol. 36, no. 1, pp. 122–130, Jan./Feb. 2000.
[15] C. Lascu, I. Boldea, and F. Blaabjerg, "Comparative study of adaptive and inherently sensorless observers for variable-speed induction-motor drives," *IEEE Trans. Ind. Electron.*, vol. 53, no. 1, pp. 57–65, Jan. 2006.
[16] M. Comanescu, L. Xu, and T. D. Batzel, "Decoupled current control of sensorless induction-motor drives by integral sliding mode," *IEEE Trans. Ind. Electron.*, vol. 55, no. 11, pp. 3836–3845, Nov. 2008.
[17] D. Traore, F. Plestan, A. Glumineau, and J. Leon, "Sensorless induction motor: High-order sliding-mode controller and adaptive interconnected observer," *IEEE Trans. Ind. Electron.*, vol. 55, no. 11, pp. 3818–3827, Nov. 2008.

Cristian Lascu received the M.S. and Ph.D. degrees in electrical engineering from the University Politehnica of Timisoara, Timisoara, Romania, in 1995 and 2002, respectively.

In 1995, he joined the Department of Electrical Engineering, University Politehnica of Timisoara, where his research was focused on power electronics and high-performance electrical drives. He was a Visiting Researcher with the Institute of Energy Technology, Aalborg University, Aalborg, Denmark, in 1997, 2005, and 2006, and with the Department of Electrical Engineering, University of Nevada, Reno, in 1999–2000 and 2007–2008. From 2002 to 2004, he was with SIEI S.p.A., Italy, working on advanced power electronics and drives for electrical vehicles under a European Marie Curie Fellowship. Since 2009, he has been with the Department of Electrical and Biomedical Engineering, University of Nevada.

Dr. Lascu received the IEEE Industry Applications Society Prize Paper Award in 1998.

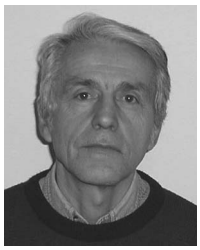

Ion Boldea (M'77–SM'81–F'96) received the B.S. and Ph.D. degrees in electrical engineering from the University Politehnica of Timisoara, Timisoara, Romania, in 1967 and 1973, respectively.

He is currently a Full Professor with the Faculty of Electrical Engineering, University Politehnica of Timisoara. He has worked and published extensively on linear and rotary electric machines and their power electronics control, with and without motion sensors. He coauthored *Induction Machine Handbook* (CRC, 2001), *Linear Motion Electromagnetic Devices* (Taylor & Francis, 2001), *Electric Drives* (CRC, 2006), and *The Electric Generators Handbook* (CRC, 2006). He spent about five years as a Visiting Scholar in the U.S. and U.K. and presented keynote addresses and intensive courses. He does consultant work in the U.S., Europe, and Asia. He is an Associate Editor of the *Electric Power Components and Systems Journal*, and the Director and Founder of the Internet-only, *Journal of Electrical Engineering*.

Dr. Boldea is an active member of the Industrial Drives and Electric Machines Committees of the IEEE Industry Applications Society. He was the Cochairman of the IEEE IAS Technically Sponsored OPTIM'96, '98, '00, '02, '04, '06, and '08 International Conferences.

Frede Blaabjerg (S'86–M'88–SM'97–F'03) was born in Erslev, Denmark, on May 6, 1963. He received the M.Sc.E.E. and Ph.D. degrees from Aalborg University, Aalborg, Denmark, in 1987 and 1995, respectively.

From 1987 to 1988, he was with ABB-Scandia, Randers, Denmark. In 2000, he was a Visiting Professor with the University of Padova, Padova, Italy, and a part-time Program Research Leader in wind turbines with the Research Center Risoe, Risoe, Italy. In 2002, he was a Visiting Professor with Curtin University of Technology, Perth, Australia. He is currently a Full Professor of power electronics and drives with the Institute of Energy Technology and the Dean of the Faculty of Engineering, Science and Medicine, Aalborg University. He is involved in research projects with industry, including the Danfoss Professor Program in Power Electronics and Drives. He is the author or coauthor of more than 350 publications in his research fields, including the book *Control in Power Electronics* (Academic, 2002). His research areas are in power electronics, static power converters, ac drives, switched reluctance drives, modeling, characterization of power semiconductor devices and simulation, power quality, wind turbines, and green power inverters.

Dr. Blaabjerg is a member of the European Power Electronics and Drives Association. He has served as a member of the Danish Technical Research Council in Denmark from 1997 to 2003, where he was the Chairman from 2001 to 2003. He has also been the Chairman of the Danish Small Satellite Program and the Center Contract Committee. He became a member of the Danish Academy of Technical Science in 2001, and in 2003, he became a member of the Academic Council. From 2002 to 2003, he was a member of the Board of the Danish Research Councils. In 2004, he became the Chairman of the Program Committee on Energy and Environment. He received the 1995 Angelos Award for his contributions to modulation technique and control of electric drives, the Annual Teacher Prize from Aalborg University in 1995, the Outstanding Young Power Electronics Engineer Award from the IEEE Power Electronics Society in 1998, five IEEE Prize Paper Awards, the C. Y. O'Connor Fellowship from Perth, Australia, in 2002, the Statoil Prize for his contributions to power electronics in 2003, and the Grundfos Prize in acknowledgment of his international scientific research on power electronics in 2004. He is an Associate Editor for the *Journal of Power Electronics* and for *Elteknik*. He has been an Associate Editor of the IEEE TRANSACTIONS ON INDUSTRY APPLICATIONS and is currently the Editor-in-Chief of the IEEE TRANSACTIONS ON POWER ELECTRONICS.